Scientific
Research
Publishing

Property and Oxidation Behaviours of (Mo,Cr)Si$_2$ + ZrO$_2$ Composite Produced by Pressure-Less Sintering

Yiming Yao[1], Erik Ström[2], Xin-Hai Li[3], Qin Lu[2]

[1]Department of Materials and Manufacturing Technology, Chalmers University of Technology, Gothenburg, Sweden
[2]Heating Systems Division, Sandvik Heating Technology AB, Hallstahammar, Sweden
[3]Material Technology, Siemens Industrial Turbomachinery AB, Finspong, Sweden
Email: yiming.yao@chalmers.se, erik.o.strom@sandvik.com, xin-hai.li@siemens.com, qin.lu@sandvik.com

Abstract

A composites of $(Mo_{0.9}Cr_{0.1})Si_2$ + 15vol% ZrO_2 was prepared with powder metallurgy and Pressure-Less Sintering (PLS) method, aiming at applications of high temperature structural materials. Mechanical properties of the composites were assessed with hardness, indentation fracture toughness K_c and K_{IC} tested using SEVNB, flexure strength at room temperature and 1200°C, and isothermal oxidation at 1400°C. The results showed that the native silica oxide and molybdenum-oxides on the silicide feedstock surface were significantly reduced in terms of Cr-alloying. $(Mo_{0.9}Cr_{0.1})Si_2$ and its composite also exhibited improved sinterability and grain growth, owing to the presence of $(Cr, Mo)_5Si_3$ at grain boundaries. Fracture toughness of the composite was increased by a factor of 1.6 to that in the monolithic silicide. Mechanical property of the composite at high temperature was not affected by Cr addition. However, the high temperature oxidation resistance was greatly improved in the $(Mo_{0.9}Cr_{0.1})Si_2$ + 15vol% ZrO_2 compared with the non Cr-alloyed counterpart. The Cr-alloying effects on the microstructure, fracture behaviour, and high temperature oxidation resistance were discussed.

1. Introduction

Molybdenum disilicide MoSi$_2$ is a candidate for high-temperature structural materials due to high melting point, high specific strength (strength/density), high thermal conductivity, and excellent oxidation resistance at elevated temperature [1]. However, the properties of fracture toughness and creep resistance have to be improved before engineering applications. Promising approaches include solid solution alloying the silicide (Al, V, Cr, Ta,

Nb, and Re, etc.), and composite reinforced with refractory and ceramic particles and fibres (SiC, Si_3N_4, Al_2O_3 and ZrO_2) [2]. Significant increasing in fracture toughness and strengthening at high temperature has been reported in $MoSi_2$-ZrO_2 composites in terms of phase transformation toughening of ZrO_2, but the degraded oxidation resistance was also observed, especially with a high ZrO_2 content [3] [4].

In this investigation, Cr alloyed molybdenum disilicide $(Mo_{0.9}Cr_{0.1})Si_2$, and composite $(Mo_{0.9}Cr_{0.1})Si_2$ + $15vol\%ZrO_2$ were produced with Pressure-Less Sintering (PLS) that was the most economic and practical technique applied popularly in industrial production. The purpose of this study is to investigate the alloying effect of Cr addition on mechanical properties and high temperature oxidation resistance in comparison with the un-alloyed $MoSi_2$ + $15vol\%ZrO_2$ composite.

2. Experimental Methods

$(Mo_{0.9}M_{0.1})Si_2$ (3.3 at%Cr) and $(Mo_{0.9}M_{0.1})Si_2$ + 15 vol%ZrO_2 composites were prepared using a powder metallurgy process described in an earlier work [4]. The average particle sizes were in a range of 2.3 - 2.6 and 0.87 μm for the Cr-alloyed silicide and un-stabilized ZrO_2 feedstocks, respectively. The powder mixture was milled in gasoline for 4 hours, and pressed to 60% of theoretical density (T.D.) using Cold Isostatic Pressing (CIP) at 200 MPa. PLS process was performed at 1600°C - 1620°C in H_2 atmosphere. The sintering density was measured using Archimedes method. Native oxides on the silicide feedstock powder surfaces were examined using X-ray Photoelectron Spectroscopy (XPS). Phases were determined using XRD with Cr-K_α radiation. The microstructure was characterized with optical microscope and scanning electron microscope (SEM) with Energy Dispersive Spectroscopy (EDS).

The fracture toughness was measured with two methods: K_c indentation fracture toughness (IF) calculated with the Anstis formula; K_{IC} fracture toughness tested with a standard method of Single Edge V-Notch Beam (SEVNB). The 4-point bending tests were conducted with inner/outer spans of 20/40 mm, and with a cross head speed was 0.2 mm/s. As-sintered surfaces from PLS remained on the testing pieces. The flexure strength was tested at room temperature and at 1200°C in ambient air. Discontinuous isothermal oxidation test was performed at 1400°C for 1000 h in flowing air. The weight changes were carefully measured after each exposure with accuracy of 0.1 mg.

3. Results and Discussion

3.1. Oxides on Stoking Powder Surfaces

Figure 1 shows XPS spectra of $MoSi_2$ and $(Mo_{0.9}Cr_{0.1})Si_2$ silicide feedstock at the Si_{2p}, Mo_{3d} and Cr_{3d}. The area ratios of Si_{2p} peaks at SiO_2 and $MoSi_2$ are 2.9 and 1.0 for the $MoSi_2$ and $(Mo_{0.9}Cr_{0.1})Si_2$ powder surfaces, respectively (**Figure 1(a)**). The area ratios of Mo_{3d} peaks at Mo-oxides and $MoSi_2$ are 1.7 and 1.0 in the $MoSi_2$ and $(Mo_{0.9}Cr_{0.1})Si_2$ powder surfaces, respectively (**Figure 1(b)**). The Cr_{2p} peak of Cr_2O_3 was found in the $(Mo_{0.9}Cr_{0.1})Si_2$ powder surface, and the area ratio of Cr_2O_3 to Cr-silicide is 1.4 (**Figure 1(c)**). It is apparent that the formation of silica and Mo-oxides on the $(Mo_{0.9}Cr_{0.1})Si_2$ powder surface are substantially impeded by the formation of Cr-oxides. The oxygen in the sintered bulk is believed to be introduced from the native oxide on the stocking powders. According to the chemical analysis, the oxygen contents were 2.16 and 1.13 wt% in the $MoSi_2$ and $(Mo_{0.9}Cr_{0.1})Si_2$ sintered bulks. Meanwhile, substantially decreasing of SiO_2 particles was observed in the sintered $(Mo_{0.9}Cr_{0.1})Si_2$ and composite bulks (see the following section). It was consistently testified that Cr-addition can efficiently reduce silica in molybdenum disilicide. It is widely agreed that low silica at grain boundaries is appreciable to the creep resistance of silicide composites [5]. Thus, Cr-alloying is an alternative approach to reduce the SiO_2 contents of silicide composites, which could contribute to creeping property at elevated temperature.

3.2. Sintering Density

Theoretical density of $MoSi_2$ and $(Mo_{0.9}Cr_{0.1})Si_2$ silicides are 6.25 and 6.10 g/cm^3, respectively, measured from XRD. Theoretical densities of $MoSi_2$ + $15vol\%ZrO_2$ and $(Mo_{0.9}Cr_{0.1})Si_2$ + $15vol\%ZrO_2$ are 6.16 and 6.04 g/cm^3, calculated from a linear combination rule. The sintering density of different materials is shown in **Table 1**. High sintering density over 98% T.D. was obtained in both Cr-alloyed silicide and composite. Improved sinterability is directly related to the existence of $(Cr, Mo)_5Si_3$ type silicide as secondary phase presenting (see the following
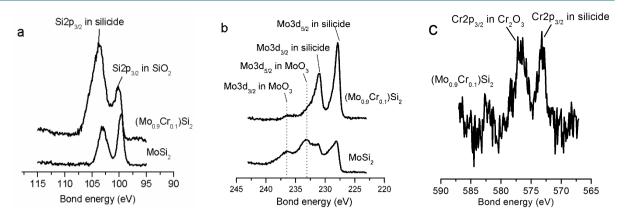
Figure 1. XPS spectra at (a) Si_{2p}; (b) Mo_{3d} in the surface of the $MoSi_2$ and $(Mo_{0.9}Cr_{0.1})Si_2$ feedstock powders, (c) Cr_{2p} in the surface of the $(Mo_{0.9}Cr_{0.1})Si_2$ feedstock powder.

Table 1. Property of sintered silicides and composites.

Materials	Sintering density (g/cm³)	Relative density (%T.D.)	Average grain size (μm)	HV10 (GPa)
$MoSi_2$	6.01	96.2	5	8.7 ± 0.3
$(Mo_{0.9}Cr_{0.1})Si_2$	6.06	99.3	14	7.7 ± 0.2
$MoSi_2 + 15vol\%ZrO_2$	5.84	95.0	4	8.7 ± 0.2
$(Mo_{0.9}Cr_{0.1})Si_2 + 15vol\%ZrO_2$	5.95	98.5	11	7.9 ± 0.2

section). The melting point of $CrSi_2$ is 1551°C, nearly 470°C lower than that of $MoSi_2$. According to a quasibinary section phase diagram of $MoSi_2$-$CrSi_2$, a peritectic reaction exists at 7 at%Cr at 1529°C, taking place as $L + Mo_{1-x}Cr_xSi_2 \Leftrightarrow Mo_yCr_{1-y}Si_2$ [6]. A liquid phase might appear at the sintering temperature, which may greatly assist mass transport and densification process during sintering at 1600°C - 1620°C.

3.3. Material Characterization

The XRD analysis shows that the $(Mo_{0.9}Cr_{0.1})Si_2$ consists of a single-phase of tetragonal $C11_b$ structure. The Cr solid solubility in the $(Mo_{0.9}Cr_{0.1})Si_2$ is 2.5 - 2.6 at% by EDS, which is lower than the nominal composition of 3.3 at%. Typical microstructures of different materials are shown in **Figure 2**. The amount of SiO_2 particles in $(Mo_{0.9}Cr_{0.1})Si_2$ was reduced to 1.4 vol% compared with 2.2 vol% in $MoSi_2$, measured from selected dense areas with imaging process. A small amount of Mo_5Si_3 was observed in MoS_2 (**Figure 2(a)**). In $(Mo_{0.9}Cr_{0.1})Si_2$, the Mo_5Si_3 phase was replaced by a Cr-rich silicide with a composition of Cr:Mo:Si = 45:15:40 (at%) close to $(Cr_{0.75}Mo_{0.25})_5Si_3$. The Cr-rich silicide appears as discrete grains and continuous phase along grain boundaries (**Figure 2(b)**). Grain growth is substantial in $(Mo_{0.9}M_{0.1})Si_2$ by a factor of 3 of that in $MoSi_2$ (**Table 2**), which could be ascribed to the liquid phase sintering effect of the existence of the $(Cr, Mo)_5Si_3$ silicide with lower melting point. ZrO_2 particles were well-dispersed in both composites (**Figure 3(c)** and **Figure 3(d)**), and grain sizes in both composites were refined owing to the dispersion of ZrO_2 particles (**Table 2**). The Mo_5Si_3 grains are still visible in $MoSi_2 + 15vol\%ZrO_2$ (**Figure 2(c)**), but the $(Cr, Mo)_5Si_3$ is hardly recognized in $(Mo_{0.9}M_{0.1})Si_2 + 15vol\%ZrO_2$ composite from the contrast in SEM images (**Figure 2(d)**).

3.4. Mechanical Property

Mechanical properties are shown in **Table 1** and **Table 2**. The average hardness values of the $(Mo_{0.9}Cr_{0.1})Si_2$ matrix phase and $(Mo_{0.9}Cr_{0.1})Si_2 + 15vol\%ZrO_2$ composite are 10% lower than their un-Cr alloyed counterparts (**Table 1**), which might result from the softening effect of the Cr-addition. The fracture toughness K_{IC} of the two composites are comparable, which are higher than the monolithic silicides in a factor of 1.4 - 1.6 (**Table 2**). The fracture toughness values from indentation fracture (K_c) and SEVBN (K_{IC}) methods are close in $MoSi_2 + 15vol\%ZrO_2$. However, the K_c value is too high over K_{IC} in the $(Mo_{0.9}Cr_{0.1})Si_2 + 15vol\%ZrO_2$ composite, which
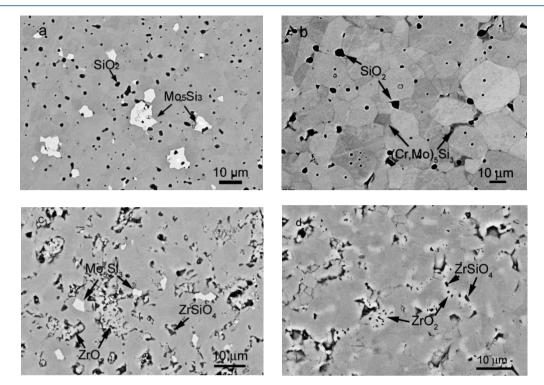
Figure 2. Microstructure of as-sintered silicides and composites (a) MoSi$_2$, (b) (Mo$_{0.9}$Cr$_{0.1}$)Si$_2$, (c) MoSi$_2$ + 15vol%ZrO$_2$, and (d) (Mo$_{0.9}$Cr$_{0.1}$)Si$_2$ + 15vol%ZrO$_2$.

Table 2. Mechanical property of silicides and composites.

Materials	K_c (98N) (MPa.m$^{1/2}$)	K_{IC} (SEVNB) (MPa.m$^{1/2}$)	σ_f (Room temp.)(MPa)	σ_f (high temp.) (MPa)
MoSi$_2$	3.0 ± 0.2	3.0 ± 0.2	450 ± 40	≥330 (1100°C)
MoSi$_2$ + 15vol%ZrO$_2$	4.7 ± 0.6	4.2 ± 0.2	325 ± 40	334 ± 14 (1200°C)
(Mo$_{0.9}$Cr$_{0.1}$)Si$_2$ + 15vol%ZrO$_2$	6.4 ± 0.4	4.7 ± 0.3	293 ± 25	200 ± 27 (1200°C)

is caused by the uncertainty in determination of the crack length. **Figure 3** shows typical indentation cracks in the composites. The primary median cracks from the indent corners in MoSi$_2$ + 15vol%ZrO$_2$ are deflected (D), branched (Bra), bridged (Bri) by the dispersed ZrO$_2$ additives (**Figure 3(a)**), which dissipates and absorbs the energy for crack propagation. In contrast, multi-cracks are developed around the indent edges in (Mo$_{0.9}$Cr$_{0.1}$)Si$_2$ + 15vol%ZrO$_2$ (**Figure 3(b)**). In such a case, the measured crack length is not reliable and inaccurate, which results in the overestimated K_c result. It is implied that the indentation fracture method is not suitable to describe the fracture toughness property of the composite (Mo$_{0.9}$Cr$_{0.1}$)Si$_2$ + 15vol%ZrO$_2$, therefore, a verification with a standard method has to be considered. The room temperature flexural strength σ_f of the composites is lower than that of MoSi$_2$ (**Table 2**). The σ_f of (Mo$_{0.9}$Cr$_{0.1}$)Si$_2$ + 15vol%ZrO$_2$is substantially reduced at 1200°C compared with MoSi$_2$ + 15vol%ZrO$_2$. It is believed that interfacial fracture energy is changed between the alloyed silicide matrix and ZrO$_2$ particles [7], and grain boundaries can be weakened by the present of the (Cr, Mo)$_5$Si$_3$ phase in (Mo$_{0.9}$Cr$_{0.1}$)Si$_2$ + 15vol%ZrO$_2$ at elevated temperatures.

3.5. High Temperature Oxidation Test

Figure 4 shows time dependence of mass change after isothermal exposure at 1400°C in air. All the samples present with parabolic kinetics in the steady oxidation stage, indicating the formation of protective oxide scales and diffusion controlled oxidation. Total weight gains in (Mo$_{0.9}$Cr$_{0.1}$)Si$_2$ and MoSi$_2$ are 1.7 and 3.6 mg/cm^2 after 1000 h exposure, inferring that the thickness of the SiO$_2$ layer on the Cr-alloyed silicide (Mo$_{0.9}$Cr$_{0.1}$)Si$_2$ is thinner than that on MoSi$_2$. The performance of (Mo$_{0.9}$Cr$_{0.1}$)Si$_2$ + 15vol%ZrO$_2$ composite is similar to that of monolithic
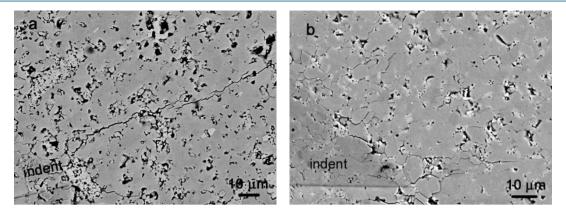
Figure 3. Cracks at indents in the composites (a) $MoSi_2$ + 15vol%ZrO_2, and (b) $(Mo_{0.9}Cr_{0.1})Si_2$ + 15vol%ZrO_2.
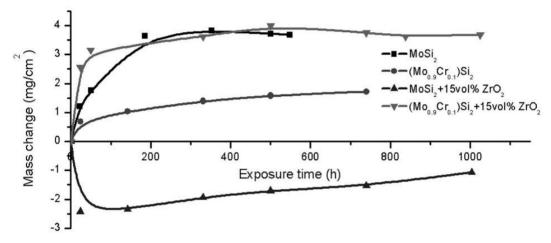

Figure 4. Exposure time dependence on weight change at 1400°C in air.

$MoSi_2$. In contrast, an erratic weight loss occurred in un-alloyed composite $MoSi_2$ + 15vol%ZrO_2 in the initial oxidation stage within 50 h. A parabolic weight-gain in $MoSi_2$ + 15vol%ZrO_2 is established when a continuous silica layer is formed. The rate constants in the steady oxidation stage (after 50 h) are 0.0014 and 0.0006 ($mg^2 \cdot cm^{-4} \cdot h^{-1}$) in $MoSi_2$ + 15vol%ZrO_2 and $(Mo_{0.9}Cr_{0.1})Si_2$ + 15vol%ZrO_2, respectively. Obviously, the oxidation rate is substantially decreased in the Cr-alloyed composite.

The oxide scales on both composites consist of tetragonal $ZrSiO_4$ and α-SiO_2 by XRD. Typical morphologies of the composite surfaces after 1000 h exposure are shown in **Figure 5**. The scale on $MoSi_2$ + 15vol%ZrO_2 surface contains large amounts of smaller zircon particles with a size of 1 - 2 μm (**Figure 5(a)**). In contrast, the surface of $(Mo_{0.9}Cr_{0.1})Si_2$ + 15vol%ZrO_2 is comprised zircon particles with a size of 3 - 5 μm (**Figure 5(c)**). Scale thickness is between 50 - 60 and 20 - 30 μm in $MoSi_2$ + 15vol%ZrO_2 and $(Mo_{0.9}Cr_{0.1})Si_2$ + 15vol%ZrO_2, respectively. SEM cross sectional images show that Mo_5Si_3 grains are located at the interface between the base silicide and oxide scale of $MoSi_2$ + 15vol%ZrO_2 (**Figure 5(b)**). The fine zircon particle network in the scale of $MoSi_2$ + 15vol%ZrO_2 can provide fast diffusion paths for oxygen to the interface of scale-base silicide, which results in higher oxidation rate. In comparison, the oxide scale of $(Mo_{0.9}Cr_{0.1})Si_2$ + 15vol%ZrO_2 consists of nearly pure silica. Some large zircon particles mainly appear on the outermost surface of this composite. A few small discrete Cr_2O_3 grains were found at the interface (**Figure 5(d)**), which resulted from the outer diffusion and oxidation of Cr from the alloyed base silicide after the formation of the protective silica scale.

It is known that the formation of protective silica on $MoSi_2$ at high temperature surface is implemented by selective oxidation of Si: $MoSi_2 + O_2 \rightarrow MoO_3(g) + SiO_2$ at high pO_2; and $MoSi_2 + O_2(g) \rightarrow Mo_5Si_3 + SiO_2$, at low pO_2. In the latter case, and silica can form at surface and Mo_5Si_3 silicide usually form at the interface between scale and base silicide as oxygen diffuses through the surface oxide layer. In presence of ZrO_2 additives, SiO_2 will react with ZrO_2 to form zircon: $SiO_2 + ZrO_2 = ZrSiO_4$, thus, the resultant zircon particles are retained in
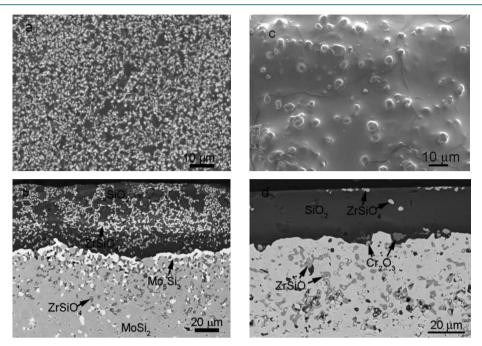
Figure 5. Plane view and cross section of the composites after exposure at 1400˚C for 1000 h, (a) and (b) $MoSi_2$ + 15vol%ZrO_2, and (c) and (d) $(Mo_{0.9}Cr_{0.1})Si_2$ + 15vol%ZO_2.

the oxide scale. The improved oxidation behaviour of the Cr- alloyed composite can be attributed to the chemistry change at the as received surfaces sintered in reduced atmosphere. It was reported that as-sintered surface of PLSed $MoSi_2$ + 15vol%ZrO_2 is comprised with a silicon depleted silicide (Mo-Zr-Si) [8]. The substantial weight loss presenting in initial oxidation occurred in this composite was ascribed to the rapid oxidation of the high Zr-content silicide in the outermost surface. In comparison, the PLS sintered $(Mo_{0.9}Cr_{0.1})Si_2$ + 15vol%ZrO_2 surface consists of Cr-rich silicide with a low Zr content. It is believed that this silicide in the as-sintered surface could assists the formation of SiO_2 scale with a favourable microstructure (showed in **Figure 5(d)**) at relative lower temperature. The outer diffusion of Cr can also promote the mobility and diffusion of Si at high temperature in the Cr-alloyed composite. The investigation details will be published in a later paper.

4. Conclusion

$(Mo_{0.9}Cr_{0.1})Si_2$ + 15vol% ZrO_2 composite with high sintering density 99% T.D. was prepared with pressure-less sintering method. The native silica and Mo-oxides in the Cr-alloyed silicide feed stocking surface was substantially reduced by means of forming Cr-oxides. As a result, the amount of silica particles in the sintered silicide bulk was reduced by 50%. The sinterablity of the composite was improved considerably due to the existence of small amounts of $(Cr_{0.75}Mo_{0.25})Si_2$ silicide at grain boundaries. Toughening effect of the composite was not influenced by Cr-addition, and flexure strength was 200 MPa at 1200˚C. However, the as-sintered $(Mo_{0.9}Cr_{0.1})Si_2$ + 15vol%ZrO_2 composite exhibited an excellent oxidation behaviour at 1400˚C, and the weight loss occurred at the starting oxidation in the as-sintered $MoSi_2$ + 15vol%ZrO_2 was avoided.

Acknowledgement

References

[1]   Vasudevan, A.K. and Petrovic, J.J. (1992) A comparative Overview of Molybdenum Disilicide Composites. *Materials Science and Engineering A*, **155**, 1-17. http://dx.doi.org/10.1016/0921-5093(92)90308-N

[2]   Waghmare, U.V., Bulatov, V., Kaxiras, E. and Duesbery, M.S. (1999) *Mater. Sci. Eng. A*, **261**, 147-157.

[3] Petrovic, J.J., Bhattacharya, A.K., Honnell, R.E. and Mitchell, T.E. (1992) ZrO_2 and ZrO_2-SiC Particle Reinforced $MoSi_2$ Matrix Composites. *Mater. Sci. Eng. A*, **155**, 259-266. http://dx.doi.org/10.1016/0921-5093(92)90332-U

[4] Gong, K., Yao, Y., Sundberg, M., Li, X-H., Ström, E. and Li, C. (2006) Toughening Effect and Oxidation Behaviour of $MoSi_2$-ZrO_2 Composites. *Pro.* 2006 *MRS Fall Meeting*, *Mater. Res. Soc. Symp. II*: *Advanced Intermetallic-Based Alloys*, Vol. 980, Boston, 0980-II05-35.

[5] Lin, G.Y. Costil, V., Jorand, Y. and Fantozzi, G. (1999) Experiments on Packing and Sintering of Composite Powder Mixtures of $MoSi_2$ + Al_2O_3 Platelets. *Ceramics International*, **25**, 367-373. http://dx.doi.org/10.1016/S0272-8842(98)00055-8

[6] Pandelaers, L. and Schmid-Fetzer, R. (2010) Chromium-Molybdenum-Silicon. Landolt-Börnstein, New Series IV/11E3, Springer, 182-191.

[7] Singh, J.P., Virkar, A.V., Shetty, D.K. and Gordow, R.S. (1978) Strength-Grain Size Relations in Polycrystalline Ceramics. *J. Am. Ceram. Soc.*, **62**, 179-183. http://dx.doi.org/10.1111/j.1151-2916.1979.tb19049.x

[8] Yao, Y., Ström, E. and Li, X. (2012) Effect of Sintering Atmosphere on Surface and High-Temperature Oxidation of Pressure-Less Sintered $MoSi_2$-ZrO_2 Composite. *Proc. International Conference on Innovative Technologies*, *IN-TECH* 2012, Rijeka, 473.

Scientific Research Publishing

Submit or recommend next manuscript to SCIRP and we will provide best service for you:

Accepting pre-submission inquiries through Email, Facebook, LinkedIn, Twitter, etc.

A wide selection of journals (inclusive of 9 subjects, more than 200 journals)

Providing 24-hour high-quality service

User-friendly online submission system

Fair and swift peer-review system

Efficient typesetting and proofreading procedure

Display of the result of downloads and visits, as well as the number of cited articles

Maximum dissemination of your research work

Submit your manuscript at: http://papersubmission.scirp.org/